

## Quantum entanglement in photon-atom scattering

K. W. Chan,<sup>1,\*</sup> C. K. Law,<sup>1,2</sup> and J. H. Eberly<sup>1</sup>

<sup>1</sup>Center for Quantum Information and Department of Physics and Astronomy, University of Rochester, Rochester, New York 14627, USA

<sup>2</sup>Department of Physics, The Chinese University of Hong Kong, NT, Hong Kong SAR, China

(Received 25 March 2003; published 27 August 2003)

Joint atom-photon states can become nonseparably entangled by momentum conservation in scattering events. The consequences are open for observation in interference experiments in which one particle is used to monitor the evolution of the other. We have previously quantified the degree of available recoil entanglement in spontaneous emission, and present here the extensions to Rayleigh scattering and Raman scattering, with an emphasis on the similarity among the three cases. It is found that such scattering processes have the potential to create a higher degree of entanglement between the scattered photon and the recoiled atom than any reported to date.

DOI: 10.1103/PhysRevA.68.022110

PACS number(s): 03.65.Ud, 42.50.Vk, 32.80.Lg

### I. INTRODUCTION

Quantum entanglement is a property shared by two or more quantum-correlated systems. Since Schrödinger introduced his cat (macroscopic quantum interference) [1], entanglement has been a continuing subject of interest during the development of quantum mechanics. It became the central topic in discussions of the completeness of quantum theory [2] after the famous paper of Einstein, Podolsky, and Rosen [3]. It is found to be crucial in the decoherence process that accounts for the classical appearance of the macroscopic world [4], as well as applications in quantum information and computation [5].

Photon entanglement is almost always discussed in finite Hilbert spaces, e.g., the state-space for two orthogonal polarization assignments used in Bell violation experiments [6,7]. Here our interest is in the nature of entanglement in continuously infinite Hilbert space, as is needed to describe processes such as single-photon emission with atomic recoil. An infinite Hilbert space provides the entangled particles with a wide range of quantum states. This makes high degrees of entanglement possible.

Generally, entanglement generated by a dynamical process originates from conservation laws. We concern ourselves here with the momentum conservation that correlates the linear momenta of an emitted photon and a recoiling atom. Such an entanglement can occur in interference experiments [8,9]. Related experimental work on atomic spontaneous emission has also been reported [10], but we have already shown that one can realistically expect very little entanglement in this case [11].

Now we extend our treatment of entanglement in spontaneous emission to the closely related processes of spontaneous Raman and Rayleigh scattering [12] as shown in Fig. 1. In this paper, we show that much stronger entanglement can be achieved in Raman and Rayleigh scattering, compared to spontaneous emission, and we explain why.

We first give a theoretical framework for the analysis of entanglement in atom-photon scattering and a review of the

recoil effect on spontaneous emission. Then the joint atom-photon probability amplitudes of Raman and Rayleigh scattering are derived. We introduce the Schmidt decomposition [13] to provide a detailed analysis following the approach of previous studies of frequency-entangled down-conversion photons [14]. Since the three processes considered in this paper share similar features in their joint atom-photon states, one can analyze their entanglement collectively.

### II. THEORETICAL FRAMEWORK

Quantum entanglement of scattering events is a reflection of the Hilbert space structure of the system. In order to determine the momentum entanglement of the atom and the scattered photon, we need to find the distribution of the momenta of the two particles after the interaction. This is conveniently accomplished in the Schrödinger picture. All the information about the Hilbert space is contained in the joint probability amplitude  $C(\mathbf{q}, \mathbf{k})$ , where  $\mathbf{q}$  and  $\mathbf{k}$  denote the wave vectors of the atom and the photon after the interaction.

Let  $\hat{\mathbf{P}}$  and  $\hat{\mathbf{R}}$  denote the center-of-mass momentum and position operators of the atom with mass  $M$ . Suppose also that the internal atomic states are given by  $|j\rangle$  with energies  $E_j$ . The Hamiltonian of the system is written as

$$\hat{H} = \frac{\hat{\mathbf{P}}^2}{2M} + \sum_j E_j |j\rangle\langle j| + \sum_s \int d^3k \hbar \omega_k \hat{a}_{ks}^\dagger \hat{a}_{ks} - \hat{\mathbf{d}} \cdot \mathbf{E}(\hat{\mathbf{R}}, t). \quad (1)$$

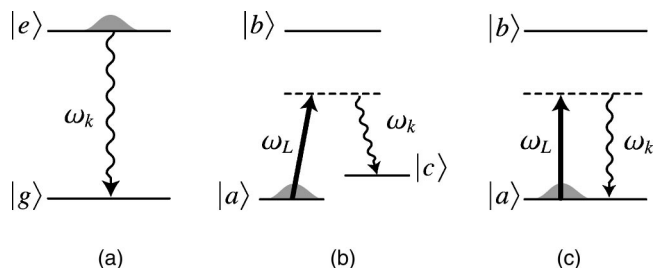


FIG. 1. The three models that involve atom-photon entanglement: (a) spontaneous emission, (b) Raman scattering, and (c) Rayleigh scattering.

\*Electronic address: kwchan1@pas.rochester.edu

The first two terms are the kinetic energy and the internal electronic state energy of the atom. The third term is the quantized electromagnetic field energy and the last term is the atom-field interaction in dipole approximation with  $\hat{\mathbf{d}}$  denoting the dipole moment operator of the atom. The electric field has possibly both classical and quantum elements:

$$\begin{aligned} E(\hat{\mathbf{R}}, t) = & \mathcal{E}(t)(e^{i(\mathbf{k}_L \cdot \hat{\mathbf{R}} - \omega_L t)} + e^{-i(\mathbf{k}_L \cdot \hat{\mathbf{R}} - \omega_L t)}) \\ & + \sum_s \int d^3 k i \sqrt{\frac{\hbar \omega_k}{2 \epsilon_0 (2\pi)^3}} \\ & \times (\mathbf{e}_{\mathbf{k}s} e^{i\mathbf{k} \cdot \hat{\mathbf{R}}} \hat{a}_{\mathbf{k}s} - \mathbf{e}_{\mathbf{k}s}^* e^{-i\mathbf{k} \cdot \hat{\mathbf{R}}} \hat{a}_{\mathbf{k}s}^\dagger). \end{aligned} \quad (2)$$

The first term represents a classical incident field and the second term is the quantized field which is responsible for spontaneous emission or scattering. Here  $a_{\mathbf{k}s}$  and  $a_{\mathbf{k}s}^\dagger$  are the annihilation and creation operators of the quantized electromagnetic field with photon wave vector  $\mathbf{k}$  and polarization  $s$ , which obey the commutation relation  $[a_{\mathbf{k}s}, a_{\mathbf{k}'s'}^\dagger] = \delta_{ss'} \delta(\mathbf{k} - \mathbf{k}')$ .

Before spontaneous decay or interaction with the laser, the electromagnetic field state is the vacuum  $|\{0\}\rangle$  and the atom is prepared in some initial state  $|a\rangle$  with center-of-mass momentum distribution given by  $a_0(\mathbf{p})$ , where  $\hbar\mathbf{p}$  is the momentum of the atom. We can write the joint atom-field state in a separable form

$$\begin{aligned} |\Psi(t=0)\rangle = & \left( \int d^3 p a_0(\mathbf{p}) |\mathbf{p}, a\rangle \right) \otimes |\{0\}\rangle \\ \equiv & \int d^3 p a_0(\mathbf{p}) |\mathbf{p}, a; \{0\}\rangle. \end{aligned} \quad (3)$$

When the emission or scattering process is completed, the atom recoils while emitting a photon. The two particles fly apart from each other and have no more interaction. However, they are entangled. Their joint probability amplitude  $C(\mathbf{q}, \mathbf{k})$  describing their momenta after the interaction is not factorable, i.e.,  $C(\mathbf{q}, \mathbf{k}) \neq f_1(\mathbf{q})f_2(\mathbf{k})$ . Hence the state is written as a double and continuously infinite nonseparable sum of joint atom-photon states

$$|\Psi(t \rightarrow \infty)\rangle = \sum_s \int d^3 q \int d^3 k C(\mathbf{q}, \mathbf{k}) |\mathbf{q}, c; 1_{\mathbf{k}s}\rangle, \quad (4)$$

where  $|c\rangle$  is the final internal (electronic) state. Note that the photon polarization index  $s$  for the amplitude  $C(\mathbf{q}, \mathbf{k})$  has been suppressed since we are only interested in the continuous variables  $\mathbf{q}$  and  $\mathbf{k}$ . We shall choose a particular polarization in detecting the photon and the explicit form of  $C$  is unaffected.

### III. SCHMIDT DECOMPOSITION

Schmidt decomposition is one of the methods used to quantify the degree of entanglement of a bipartite system in a pure state [13]. By applying the decomposition, the ampli-

tude  $C(\mathbf{q}, \mathbf{k})$  can be converted into a discrete sum of factored products uniquely:

$$C(\mathbf{q}, \mathbf{k}) = \sum_n \sqrt{\lambda_n} \psi_n(\mathbf{q}) \phi_n(\mathbf{k}), \quad (5)$$

where  $\lambda_n$  and  $\phi_n(\mathbf{k})$  are the eigenvalues and eigenfunctions of the integral equation

$$\int d^3 k' \rho^F(\mathbf{k}, \mathbf{k}') \phi_n(\mathbf{k}') = \lambda_n \phi_n(\mathbf{k}), \quad (6)$$

with the photon density matrix defined by

$$\rho^F(\mathbf{k}, \mathbf{k}') \equiv \int d^3 q C(\mathbf{q}, \mathbf{k}) C(\mathbf{q}, \mathbf{k}')^*. \quad (7)$$

Because the  $\lambda$ 's are the eigenvalues of the photon density matrix, we have  $\sum \lambda_n = 1$ , and the  $\phi(\mathbf{k})$ 's form a complete orthonormal set of photon wave functions.  $\psi_n(\mathbf{q})$  is the corresponding normalized atom eigenfunction related to  $\phi_n(\mathbf{k})$  through

$$\psi_n(\mathbf{q}) = \frac{1}{\sqrt{\lambda_n}} \int d^3 k C(\mathbf{q}, \mathbf{k}) \phi_n(\mathbf{k})^*. \quad (8)$$

It is equally good to obtain all the eigenvalues and eigenfunctions through the atom density matrix, and they are the same as those derived from the photon density matrix. Equation (8) serves to fix the relative phase of the atom and photon eigenmodes.

The decomposition in Eq. (5) has three important properties. First, as noted above, it provides a complete set of orthonormal functions  $\phi_n(\mathbf{k})$  for the photon specific to the emission or scattering process. Second, it pairs an atom mode  $\psi_n(\mathbf{q})$  with its photon counterpart  $\phi_n(\mathbf{k})$  in a unique way. Third, the basis of the decomposition is explicitly discrete, in contrast to the original continuous momentum space bases used to describe the state vector.

Naturally discreteness allows the Schmidt modes to be counted. Now the eigenvalues can be ordered according to  $\lambda_1 \geq \lambda_2 \geq \lambda_3 \geq \dots$ , and the degree of entanglement of the two systems is obviously related to the number of  $\lambda$ 's that are "important." As a numerical measure of entanglement we will use the so-called Schmidt number [5] or participation ratio, denoted by  $K$  [15]:

$$K \equiv \frac{1}{\sum_n \lambda_n^2} \geq 1. \quad (9)$$

As an example, if  $K=1$ , the Schmidt sum has only one term and the state is not entangled. On the other hand, if there are  $N$  states all with  $\lambda_n = 1/N$ , then  $K=N$ . This explains why  $K$  is called the Schmidt number: it counts the states that are significant in making up  $|\Psi\rangle$ . It is this last feature that makes the Schmidt number more useful than other measures of entanglement (such as entropy). The number of active or im-

portant modes can be an essential parameter for an experimenter wanting to know how many modes to prepare for when designing a laboratory setup.

We now study the three photon-atom interactions: spontaneous emission, Rayleigh scattering, and Raman scattering. The strong analogies among them enable us to analyze their entanglement information together.

#### IV. SPONTANEOUS EMISSION

The first model to analyze is spontaneous radiative decay as sketched in Fig. 1(a). The Hamiltonian that describes the free-space spontaneous emission of a two-level atom with mass  $M$ , transition frequency  $\omega_0$ , and ground state and excited state  $|g\rangle$  and  $|e\rangle$  can be written as

$$\hat{H} = \frac{\hat{\mathbf{p}}^2}{2M} + \hbar\omega_0|e\rangle\langle e| + \sum_s \int d^3k \hbar\omega_k \hat{a}_{ks}^\dagger \hat{a}_{ks} + \hbar \sum_s \int d^3k [g_s(\mathbf{k})|g\rangle\langle e| \hat{a}_{ks}^\dagger e^{-i\mathbf{k}\cdot\hat{\mathbf{R}}} + \text{H.c.}]. \quad (10)$$

Note that the ground-state energy of the atom is set to zero. The coupling strength is expressed as  $g_s(\mathbf{k}) = i\sqrt{\omega_k/2\hbar\epsilon_0(2\pi)^3} \boldsymbol{\epsilon}_{ks} \cdot \mathbf{d}_{ge}$ , with  $\boldsymbol{\epsilon}_{ks}$  and  $\mathbf{d}_{ge}$  denoting the polarization of the photon and the dipole matrix element of the atom.

Initially the atom is prepared in the excited state. Then the atom recoils while dropping into the ground state. At the time  $t \gg \gamma^{-1}$  where  $\gamma$  is the natural decay rate of the upper atomic level, the state of the system can be written as

$$|\Psi(t)\rangle \rightarrow \sum_s \int d^3q \int d^3k C(\mathbf{q}, \mathbf{k}) e^{-i(T_q + kc)t} |\mathbf{q}, g\rangle \otimes |1_{ks}\rangle. \quad (11)$$

Here we denote the state of the decayed atom with final momentum  $\hbar\mathbf{q}$  by  $|\mathbf{q}, g\rangle$  and that of the emitted photon with wave vector  $\mathbf{k}$  by  $|1_{ks}\rangle$ . The joint amplitude  $C(\mathbf{q}, \mathbf{k})$  gives the correlation between the two particles.

According to Rzażewski and Żakowicz [16], the amplitude is given by

$$C^{\text{SE}}(\mathbf{q}, \mathbf{k}) = \frac{g_s(\mathbf{k})a_0(\mathbf{q} + \mathbf{k})}{T_q - T_{q+\mathbf{k}} + kc - \omega_0 + i\gamma}, \quad (12)$$

which is not factorable. Now we take the initial momentum distribution of the center of mass of the atom in its excited state to have a Gaussian shape with width  $\sigma_p$ :

$$a_0(\mathbf{p}) = \frac{1}{\sqrt{\pi}\sigma_p} \exp\left[-\left(\frac{\mathbf{p}}{\sigma_p}\right)^2\right]. \quad (13)$$

Such a momentum distribution corresponds to an atom prepared in a thermal state with zero initial mean velocity. The symbol  $T_p \equiv (\hbar\mathbf{p})^2/2M\hbar$  is a shorthand for the kinetic energy of the atom with momentum  $\hbar\mathbf{p}$  in frequency units.

The absolute square of  $C^{\text{SE}}(\mathbf{q}, \mathbf{k})$  tells us the probability of finding the atom and photon having wave vectors  $\mathbf{q}$  and  $\mathbf{k}$ .

The fact that this expression of the joint amplitude cannot be written as a product of two functions, each of which involves  $\mathbf{k}$  or  $\mathbf{q}$  alone, means that the photon and the atom are entangled in the final stage of emission.

#### V. RAMAN AND RAYLEIGH SCATTERING

Similar to the single-photon spontaneous emission considered in the last section, Raman and Rayleigh scattering also give rise to entangled atom-photon pairs enforced by momentum conservation. We shall consider them in greater detail in this section. The main difference now is the introduction of a pump field to excite the atom.

As usual, we have in mind that Raman and Rayleigh scattering both occur without populating the upper atomic level (to avoid encountering the case of fluorescence again), and so we will always take the detuning of the pump field from its one-photon resonance to be much larger than the upper level linewidth  $\gamma$ .

The schematic diagrams of Raman and Rayleigh scattering are shown in Figs. 1(b) and 1(c). These two processes are similar except that the former is inelastic while the latter is elastic. One can treat these two processes together when the final state of the atom is taken care of.

The Hamiltonian of Raman scattering is

$$\hat{H} = \frac{\hat{\mathbf{p}}^2}{2M} + E_a|a\rangle\langle a| + E_b|b\rangle\langle b| + E_c|c\rangle\langle c| + \sum_s \int d^3k \hbar\omega_k \hat{a}_{ks}^\dagger \hat{a}_{ks} - \hat{\mathbf{d}} \cdot \mathbf{E}(\hat{\mathbf{R}}, t), \quad (14)$$

in which the electric field is given by Eq. (2). For Rayleigh scattering, one can simply drop the term  $E_c|c\rangle\langle c|$  in  $\hat{H}$ .

At the same time, we restrict the state of the system to be, for Raman scattering,

$$|\Psi(t)\rangle_{\text{Ram}} = \int d^3p a(\mathbf{p}; t) |a, \mathbf{p}; \{0\}\rangle + \int d^3p b(\mathbf{p}; t) |b, \mathbf{p}; \{0\}\rangle + \sum_s \int \int d^3p d^3k c(\mathbf{p}, \mathbf{k}; t) |c, \mathbf{p}; 1_{ks}\rangle, \quad (15)$$

whereas for Rayleigh scattering

$$|\Psi(t)\rangle_{\text{Ray}} = \int d^3p a(\mathbf{p}; t) |a, \mathbf{p}; \{0\}\rangle + \int d^3p b(\mathbf{p}; t) |b, \mathbf{p}; \{0\}\rangle + \sum_s \int \int d^3p d^3k c(\mathbf{p}, \mathbf{k}; t) |a, \mathbf{p}; 1_{ks}\rangle. \quad (16)$$

Physically, it means that our analysis is confined to a two-photon process, i.e., the atom, initially in a stable state  $|a, \mathbf{p}\rangle$ , is excited to  $|b, \mathbf{p}\rangle$  by the laser beam and emits a photon  $|1_{ks}\rangle$  upon going to another stable state  $|a, \mathbf{p}\rangle$  or  $|c, \mathbf{p}\rangle$ . The non-resonant two-photon process involving intermediate states of an excited atom with an emitted photon is neglected. We shall consider the Raman scattering first and give the result for Rayleigh scattering at the end of this section.

For Raman scattering, the equations of motion of the amplitudes can be simplified by using the slowly varying variables  $u$ ,  $v$ , and  $w$ :

$$a(\mathbf{p};t) = u(\mathbf{p};t) \exp[-i(T_p + \omega_a)t],$$

$$b(\mathbf{p};t) = v(\mathbf{p};t) \exp[-i(T_{p-k_L} + \omega_a + \omega_L)t],$$

$$c(\mathbf{p}, \mathbf{k};t) = w(\mathbf{p}, \mathbf{k};t) \exp[-i(T_{p-k_L+k} + \omega_a + \omega_L)t].$$

Under the rotating-wave approximation, the equations of motion become

$$\dot{u}(\mathbf{p};t) = \frac{i}{2} \Omega(t) v(\mathbf{p} + \mathbf{k}_L; t),$$

$$\dot{v}(\mathbf{p} + \mathbf{k}_L; t) = -i D_{ba} v(\mathbf{p} + \mathbf{k}_L; t) + \frac{i}{2} \Omega(t)^* u(\mathbf{p}; t)$$

$$- \sum_s \int d^3k g_s(\mathbf{k}) w(\mathbf{p} + \mathbf{k}_L - \mathbf{k}, \mathbf{k}; t),$$

$$\dot{w}(\mathbf{p} + \mathbf{k}_L - \mathbf{k}, \mathbf{k}; t) = -i D_{ca}^k w(\mathbf{p} + \mathbf{k}_L - \mathbf{k}, \mathbf{k}; t) + g_s^*(\mathbf{k}) v(\mathbf{p} + \mathbf{k}_L; t),$$

where  $g_s(\mathbf{k}) = i \sqrt{\omega_k/2\hbar} \epsilon_0 (2\pi)^3 \boldsymbol{\epsilon}_{k_s} \cdot \mathbf{d}_{bc}$  and  $\Omega(t) \equiv 2\mathbf{d}_{ab} \cdot \boldsymbol{\mathcal{E}}(t)/\hbar$  are the coupling strength and Rabi frequency. The generalized detuning frequencies  $D_{ba}$  and  $D_{ca}^k$  are defined as

$$D_{ba} = T_{p+k_L} - T_p + \omega_{ba} - \omega_L$$

and

$$D_{ca}^k = T_{p+k_L-k} - T_p + \omega_{ca} - \omega_L + \omega_k.$$

In the Born-Markov approximation,  $v(\mathbf{p} + \mathbf{k}_L; t') \approx v(\mathbf{p} + \mathbf{k}_L; t) e^{iD_{ba}(t-t')}$ . This gives

$$\dot{v}(\mathbf{p} + \mathbf{k}_L; t) = -i(D'_{ba} - i\gamma) v(\mathbf{p} + \mathbf{k}_L; t) + \frac{i}{2} \Omega(t)^* u(\mathbf{p}; t),$$

where  $D'_{ba} = D_{ba} - \Delta\epsilon$ . The frequency shift and linewidth  $\Delta\epsilon$  and  $\gamma$  are explicitly given by

$$\Delta\epsilon = \sum_s |g_s|^2 \left( \frac{\mathcal{P}}{T_{p+k_L-k} - T_{p+k_L} + \omega_{cb} + \omega_k} \right)$$

and

$$\gamma = \sum_s \pi |g_s|^2 \delta(T_{p+k_L-k} - T_{p+k_L} + \omega_{cb} + \omega_k).$$

Note that according to the remark at the beginning of this section, we have  $|D| \gg \gamma$ ,  $\Delta\epsilon$  for both  $D_{ba}$  and  $D_{ca}^k$ .

For weak  $\Omega(t)$ , an adiabatic solution is appropriate for  $v(\mathbf{p} + \mathbf{k}_L; t)$ :

$$v(\mathbf{p} + \mathbf{k}_L; t) \approx \frac{\Omega(t)^*}{2(D'_{ba} - i\gamma)} u(\mathbf{p}; t).$$

As a result, for a long-pulse or continuous-wave laser, i.e.,  $\Omega(t) \approx \Omega = \text{const}$ , we have these solutions

$$u(\mathbf{p}; t) = a_0(\mathbf{p}) e^{-Rt},$$

$$v(\mathbf{p} + \mathbf{k}_L; t) = \frac{\Omega^* a_0(\mathbf{p})}{2(D'_{ba} - i\gamma)} e^{-Rt},$$

$$w(\mathbf{p} + \mathbf{k}_L - \mathbf{k}, \mathbf{k}; t) = \frac{-i g_s(\mathbf{k})^* \Omega^*}{2(D'_{ba} - i\gamma)} \left[ \frac{a_0(\mathbf{p})}{D_{ca}^k - iR} \right] \times \{e^{-Rt} - e^{-iD_{ca}^k t}\}, \quad (17)$$

in which we have introduced the complex absorption rate  $R$  in a weak field:

$$R = \frac{|\Omega|^2}{4} \left( \frac{1}{\gamma + iD'_{ba}} \right). \quad (18)$$

We are interested in the entanglement of the scattered photon and the recoiled atom. Therefore, when a photon is scattered, i.e.,  $t \gg |R|^{-1} > |2D'_{ba}/\Omega|^2 \gamma^{-1}$ ,

$$c(\mathbf{q}, \mathbf{k}; t) \rightarrow \frac{i g_s(\mathbf{k})^* \Omega^*}{2(D'_{ba} - i\gamma)} \frac{a_0(\mathbf{q} + \mathbf{k} - \mathbf{k}_L)}{D_{ca}^k - iR} e^{-i(T_{\mathbf{q}} + \omega_c + \omega_k)t}, \quad (19)$$

where the recoil wave vector of the atom  $\mathbf{q} = \mathbf{p} + \mathbf{k}_L - \mathbf{k}$  is used. For Raman or Rayleigh scattering, the detuning  $\Delta \equiv \omega_{ba} - \omega_L$  is much larger than the natural linewidth  $\gamma$ , and the recoil is a small perturbation. Moreover, the factor  $1/(D'_{ba} - i\gamma)$  appearing in Eq. (19) is not a resonant term; we can treat it as a smooth function of  $\mathbf{q}$  and  $\mathbf{k}$ . Consequently, Eq. (19) can take a simpler form

$$C^{\text{Ram}}(\mathbf{q}, \mathbf{k}) = \frac{G_s(\mathbf{k}) a_0(\mathbf{q} + \mathbf{k} - \mathbf{k}_L)}{T_{\mathbf{q}} - T_{\mathbf{q} + \mathbf{k} - \mathbf{k}_L} + (k c - \omega_L) - \tilde{\omega}_{ac} + i \left| \frac{\Omega}{2\Delta} \right|^2 \gamma}, \quad (20)$$

in which  $G_s(\mathbf{k}) \equiv i g_s(\mathbf{k})^* \Omega^*/2(\Delta - i\gamma)$ . Note that the time-dependent phase has been taken away since it does not contribute to entanglement, and we have introduced the Stark-shifted transition frequency  $\tilde{\omega}_{ac} \equiv \omega_{ac} - |\Omega|^2/4\Delta$ . Now Eq. (20) looks very similar to Eq. (12) if we define the effective photon wave vector and frequency

$$\Delta \mathbf{k} \equiv \mathbf{k} - \mathbf{k}_L$$

and

$$\Delta \omega \equiv k c - \omega_L, \quad (21)$$

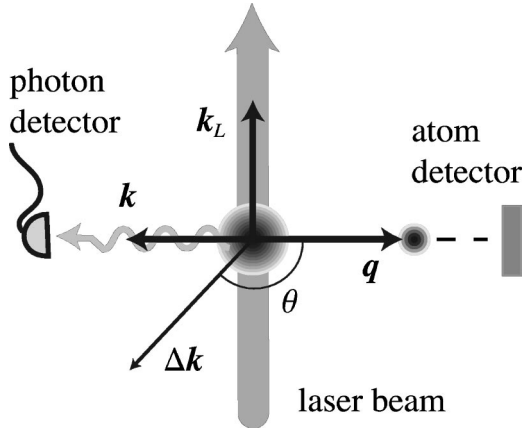


FIG. 2. Schematic diagram of the detection of the atom and the photon.

and identify  $\omega_{ac}$  and  $|\Omega/2\Delta|^2\gamma$  with  $\omega_0$  and  $\gamma$ . We shall discuss this point in more detail in the following section. For Rayleigh scattering, it is not difficult to get a similar result:

$$C^{\text{Ray}}(q, k) = \frac{G_s(k)a_0(q+k-k_L)}{T_q - T_{q+k-k_L} + \left(kc - \omega_L + \frac{|\Omega|^2}{4\Delta}\right) + i \left|\frac{\Omega}{2\Delta}\right|^2 \gamma}. \quad (22)$$

The initial momentum distribution  $a_0(p)$  can be modeled by the same Gaussian distribution as in Eq. (13).

## VI. DETECTION OF THE ATOM AND THE PHOTON

The three-dimensional models presented in the previous sections are difficult to tackle. Here we simplify the problem by restricting our attention to the detection of the photon wave vector  $k$  in a fixed direction with respect to the atom wave vector  $q$  (see Fig. 2). Such a setup is intended to suggest a class of possible experiments.

After dropping the notation of the final state, the photon + atom state is written as

$$|\Psi_\theta\rangle = \int dq \int dk C_\theta(q, k) e^{-i(T_q + kc)t} |q; 1_k\rangle. \quad (23)$$

As mentioned by the end of Sec. II, we assume that the photon is detected in a particular polarization state and so the index  $s$  in  $C_\theta$  is now a given parameter. For spontaneous emission, according to Eq. (12), if we set  $\hat{q} \cdot \hat{k} = \cos \theta$ , the amplitude reads as

$$C_\theta^{\text{SE}}(q, k) = \frac{N e^{-[q^2 + 2kq \cos \theta + k^2]/\sigma_p^2}}{\frac{-\hbar}{2M} (2kq \cos \theta + k^2) + kc - \omega_0 + i\gamma}. \quad (24)$$

The factor  $N = g_s(k)/\sqrt{\pi}\sigma_p$  is a slowly varying function of  $k$  since the probability amplitude is confined in a narrow width governed by the radiative rate  $\gamma$  which is much smaller than the resonant frequency. Therefore we can simply regard  $N$  as a constant.

It is noticed that the Compton wave vector  $Mc/\hbar$  for the atom is the largest relevant measure of momentum by a wide margin, and the decay “wave vector”  $\gamma/c$  is the smallest. We have this set of inequalities among wave vectors

$$Mc/\hbar \gg \omega_0/c, \quad \sigma_p, \quad q, \quad k \gg \gamma/c, \quad (25)$$

and we will use them to reduce the complexity of the  $q$  and  $k$  dependences of  $C_\theta(q, k)$ .

First, the narrow width of the sharp decay resonance of the denominator of  $C_\theta$  allows us to replace  $k$  by  $k_0 = \omega_0/c$  in the very small first term in the denominator, which becomes

$$\frac{-\hbar}{2M} (2k_0q \cos \theta + k_0^2) + kc - \omega_0 + i\gamma,$$

so that the amplitude is approximated as

$$C_\theta^{\text{SE}}(q, k) \approx \frac{N e^{-[q^2 + 2k_0q \cos \theta + k_0^2]/\sigma_p^2}}{-qv_R \cos \theta + kc - \left(\omega_0 + \frac{\hbar k_0^2}{2M}\right) + i\gamma}, \quad (26)$$

with  $v_R \equiv \hbar k_0/M$  denoting the mean recoil velocity of the atom. Note the symmetric role played by the variables  $q$  and  $k$  in Eq. (26). Second, we focus on the case when  $\sigma_p c \gg \gamma$  (one may also consider the other extreme in which  $\sigma_p c \ll \gamma$ ) and so the same step can be applied to the exponential

$$\exp\left[-\frac{(q + k_0 \cos \theta)^2 + (k_0^2) \sin^2 \theta}{\sigma_p^2}\right].$$

Third, we adopt a uniform normalization to the radiative width  $\gamma$  and define the “reduced” wave vectors

$$\delta q \equiv \frac{v_R}{\gamma} (q + k_0 \cos \theta), \quad (27)$$

$$\delta k \equiv \frac{1}{\gamma} \left(kc - \omega_0 + \frac{\hbar k_0^2}{2M} \cos 2\theta\right).$$

Then the final expression can be written as

$$C_\theta^{\text{SE}}(q, k) \approx \frac{N' \exp(-\delta q^2/\eta^2)}{\delta k - \delta q \cos \theta + i}, \quad (28)$$

where

$$N' = \frac{N}{\gamma} \exp\left[-\left(\frac{k_0 \sin \theta}{\sigma_p}\right)^2\right],$$

and  $\eta$  is a control parameter defined as

$$\eta \equiv \frac{\hbar k_0 \sigma_p}{M \gamma}. \quad (29)$$

Note that  $\eta$  contains all the physical parameters that determine the nature of the atomic system. As shown in Eq. (28), it controls the range of values of the scaled variable  $\delta q$  that give significant contributions to the probability amplitude.

Thus  $\eta$  serves as an ‘‘observability index.’’ If we write  $\hbar\sigma_p/M$  as velocity dispersion  $\sigma_v$  and replace  $\sigma_v/c$  by  $\sigma_\omega/\omega_0$  (the corresponding relative Doppler width of the atomic transition that would be associated with the velocity spread), we get  $\eta = \sigma_\omega/\gamma$ , which can then be interpreted as the ratio of motional to radiative linewidths. We shall also see that it is directly related to the participation ratio  $K$ .

Equation (28) represents a general class of two-body amplitudes associated with atomic spontaneous decay. The correlation between the photon and the atom enters through the Lorentzian term, which arises from energy conservation. The Gaussian indicates the range of the amplitude  $C_\theta(q, k)$ , in dimensionless units appropriately defined by the system. The combined Lorentzian-Gaussian form of Eq. (28) also appears in the absorption line shape for an atomic gas [17]. In such a system, the Gaussian arises from the Doppler shift of the resonance response frequency of an individual atom, whereas the Lorentzian comes from the collisions of the gas atoms.

By the same argument, one may obtain a similar expression for the Raman (or Rayleigh) scattering. In view of Eqs. (12) and (20), and using Eq. (21), we get

$$C_\theta^{\text{Ram}}(q, k) \approx \frac{N'' \exp(-\delta q^2/\eta^2)}{\delta k - \delta q \cos \theta + i \left| \frac{\Omega}{2\Delta} \right|^2}, \quad (30)$$

where  $\delta q$  and  $\delta k$  take the same form as those in Eq. (27), except that  $k_0$  and  $\omega_0$  are replaced by  $\Delta k_0$  and  $\tilde{\omega}_{ca}$ , respectively, and that the angle  $\theta$  is taken to be the one between the atom wave vector  $\mathbf{q}$  and the effective photon wave vector  $\Delta \mathbf{k} = \mathbf{k} - \mathbf{k}_L$ . Now  $\Delta k_0$  is defined at the value of  $k$  when the amplitude  $C^{\text{Ram}}$  takes a sharp resonance at  $\Delta \omega = \tilde{\omega}_{ac}$ . The possibility that  $\mathbf{k}$  and  $\mathbf{k}_L$  do not necessarily align ( $\Delta k_0 \neq \Delta \omega/c$ ) is reflected in the factor

$$N'' = \frac{G_s}{\sqrt{\pi}\sigma_p\gamma} \exp\left[\left(\frac{\Delta k_0 \sin \theta}{\sigma_p}\right)^2 \left(1 - \frac{2\tilde{\omega}_{ca}}{\Delta k_0 c}\right)\right],$$

which is unimportant in subsequent analysis.

Now both Eqs. (28) and (30) exhibit identical character. However, in the latter case, one can obtain a much sharper

resonance by controlling the ratio  $|\Omega/2\Delta|$  via the Rabi frequency and the laser detuning.

The control parameter  $\eta$  appearing in Eqs. (28) and (30) gives a useful entanglement measure. In the case of scattering, both the incident laser field strength and the relative orientation of  $\mathbf{k}$  and  $\mathbf{k}_L$  provide extra degrees of freedom in determining this parameter. We can see that Eq. (28) can also be used to describe Eq. (30) if we introduce the effective Rayleigh/Raman control parameter

$$\eta_R \equiv \eta \left| \frac{2\Delta}{\Omega} \right|^2, \quad (31)$$

and rescale  $\delta q$  and  $\delta k$  accordingly. In this way one may analyze the two processes together.

As a remark, the dependence of  $C_\theta$  on  $\theta$  for both spontaneous emission and scattering shows that only the projection of  $\mathbf{k}$  (or  $\Delta \mathbf{k}$ ) on  $\mathbf{q}$  is relevant to entanglement. Apparently, for Raman and Rayleigh scattering, when the incident laser is given, fixing the position of the photon detector and fixing the angle  $\theta$  in the analysis are incompatible with each other, because photons with different wave vectors recorded by the detector actually have  $\Delta \mathbf{k}$  with different  $\theta$  with respect to  $\mathbf{q}$ . However, such a variation can be neglected as the scattered photons usually have frequency very close to the resonant  $\Delta \omega \approx \tilde{\omega}_{ac}$  even though  $\mathbf{k}$  and  $\mathbf{k}_L$  are not collinear. Therefore we can focus on a particular angle  $\theta$  in subsequent analysis. We choose  $\theta = \pi$  so that the entanglement is the largest.

## VII. ENTANGLEMENT INFORMATION

After deriving the joint probability amplitudes for spontaneous emission, Raman and Rayleigh scattering, we may analyze the correlation between the atom and the photon quantitatively by means of the Schmidt decomposition. We take the angle  $\theta$  between the atom and photon wave vectors to be  $\pi$ . First, the partial density matrices of the emitted photon and the recoiled atom are determined. We notice that the symmetric role of  $q$  and  $k$  in the amplitude  $C$  under the sharp resonance condition is revealed in Eq. (26), using which the photon and atom density matrices are found to be

$$\rho^F(k_1, k_2) \equiv \int_{-\infty}^{\infty} dq C(q, k_1) C(q, k_2)^* \approx \int_{-\infty}^{\infty} dq \frac{|N|^2 e^{-[q-k_1/\sigma_p]^2} e^{-[q-k_2/\sigma_p]^2}}{\left[ v_R q + c k_1 - \left( \omega_0 + \frac{\hbar k_0^2}{2M} \right) + i\gamma \right] \left[ v_R q + c k_2 - \left( \omega_0 + \frac{\hbar k_0^2}{2M} \right) - i\gamma \right]} \quad (32)$$

and

$$\rho^A(q_1, q_2) \equiv \int_{-\infty}^{\infty} dk C(q_1, k) C(q_2, k)^* \approx \int_{-\infty}^{\infty} dk \frac{|N|^2 e^{-[q_1-k/\sigma_p]^2} e^{-[q_2-k/\sigma_p]^2}}{\left[ v_R q_1 + c k - \left( \omega_0 + \frac{\hbar k_0^2}{2M} \right) + i\gamma \right] \left[ v_R q_2 + c k - \left( \omega_0 + \frac{\hbar k_0^2}{2M} \right) - i\gamma \right]}. \quad (33)$$

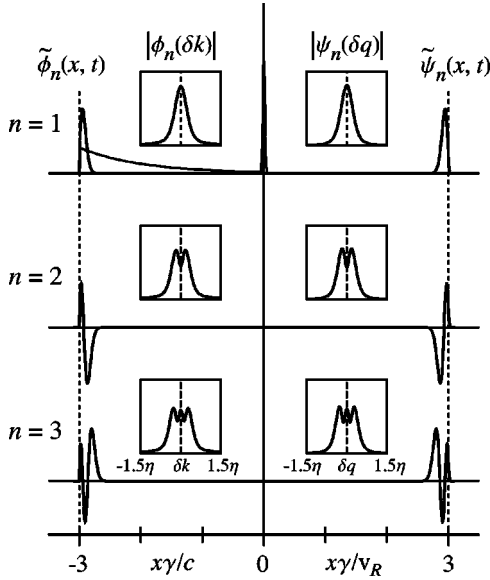


FIG. 3. The first three Schmidt pairs with  $\eta=100$ . The left and right columns give the envelopes of the photon and atom modes in position space at the time  $t=3\gamma^{-1}$ , with insets showing the corresponding modes in momentum space. Note that the spatial axes of the atom and photon modes are in different dimensionless units. The first row also shows the sharp atom state and the slowly decaying photon state in the zero recoil limit, which are plotted using the same scale as the entangled case.

By a partial fraction expansion these integrals can be written in terms of a sum of two Faddeeva functions or complex error functions if desired.

The eigenvalues  $\lambda_n$  and Schmidt functions  $\psi_n(k)$  of the photon density matrix in Eq. (32) are obtained by solving the integral equation in Eq. (6) and the corresponding atom Schmidt modes through Eq. (8). We have used matrices of size  $5000 \times 5000$  to carry out the diagonalization. Caution has to be taken in the large  $\eta$  regime when the density matrices become very sharp and localized along the diagonal. The spatial behavior of the Schmidt wave functions can also be studied by taking Fourier transforms

$$\tilde{C}(x,y;t) = \int_{-\infty}^{\infty} dq \int_{-\infty}^{\infty} dk C(q,k) e^{-i(T_q t + qx)} e^{-ik(ct-y)}. \quad (34)$$

Plots of the first three Schmidt modes with  $\eta=100$  are shown in Fig. 3. It is obvious that the atom and photon modes are nearly exactly the same except that  $\tilde{\phi}_n(x,t)=0$  for  $|x|>ct$  when the photon is not emitted. This sharp cutoff of the spatial photon modes can be seen from Eq. (32) since the Lorentzian is assumed to be much sharper than the Gaussian when we apply the inequalities in Eq. (25), whereas for the atom modes Eq. (33) suggests that the Lorentzian is sharper than the Gaussian only when  $\gamma/v_R \ll \sigma_p$ , or equivalently  $\eta \gg 1$ . Therefore the atom modes become identical to the photon modes in the large  $\eta$  limit. Also note that the number of nodes in position space (or the number of bumps in momentum space) is proportional to the Schmidt mode index  $n$ . More surprisingly, the tails of the

photon Schmidt wave functions in position space behave as Gaussians. This phenomenon corresponds to a stronger form of localization than one expects from exponential decay.

As a remark, we have ignored the dispersion effect of the atomic wave function when  $\Gamma t \gg 1$  in Fig. 3, where  $\Gamma = \hbar \sigma_p^2 / 2M$  is the dispersion rate and  $t$  is the time when the wave function is registered, since the entanglement between the individual particles is fixed once their interaction is turned off. This can be seen more explicitly by first writing the amplitude  $C(q,k)$  in Schmidt form,

$$C(q,k) = \sum_n \sqrt{\lambda_n} \psi_n(q) \phi_n(k). \quad (35)$$

Then, using Eq. (34), the corresponding position space amplitude is

$$\tilde{C}(x,y;t) = \sum_n \sqrt{\lambda_n} \tilde{\psi}_n(x;t) \tilde{\phi}_n(y-ct), \quad (36)$$

where

$$\tilde{\psi}_n(x;t) \equiv \int dq \psi_n(q) e^{-i(qx + T_q t)},$$

$$\tilde{\phi}_n(y) \equiv \int dk \phi_n(k) e^{iky}. \quad (37)$$

It can then be shown easily that  $\{\tilde{\psi}_n\}$  and  $\{\tilde{\phi}_n\}$  also form orthonormal bases for the Hilbert spaces of the atom and photon. As a result, Eq. (36) is still a Schmidt decomposition with the same  $\lambda$ 's as before, and the entanglement is not changed by the dispersion of the atomic wave packet.

## VIII. EXPERIMENTAL PARAMETERS FOR HYPERENTANGLEMENT

The relation between the Schmidt number  $K$  and the control parameter  $\eta$  is given in Fig. 4. It is found empirically that  $K \approx 1 + 0.28(\eta - 1)$  when  $\eta \gg 1$ , and that the numerical factor 0.28 depends on the form of the initial atomic momentum distribution. For the spontaneous decay of a sodium atom, one finds that  $K$  is of the order of unity [11]. Here we are interested in ways to reach much larger values, and the context of Raman scattering from cesium atoms appears realistic.

In the case of Raman and Rayleigh scattering, the effective control parameter  $\eta_R$  can be changed arbitrarily by tuning the Rabi frequency of the incident laser and its detuning with the atom. However, there are two competing practical considerations that constrain the range of attainable  $\Omega$  and  $\Delta$ . First, the atom has to interact with the laser field long enough to yield a scattered photon. This means either the atom has to move slowly or the laser beam be made wide enough, such that the interaction time is about several decay times  $\tau_R \equiv \gamma_R^{-1} = (2\Delta/\Omega)^2 \gamma^{-1}$ . On the other hand, the

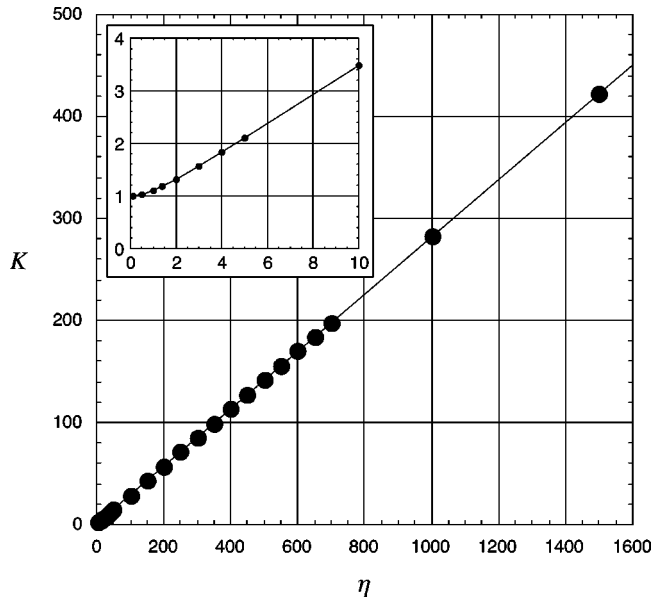


FIG. 4. The plot of the participation ratio  $K$  as a function of the control parameter  $\eta$ . The inset is a magnification of the graph near  $\eta=0$ .

power of lasers used in quantum optics experiments is usually not too large, say of the order of  $100 \text{ W/cm}^2$ .

For cesium, the atom has mass  $M=2.21 \times 10^{-25} \text{ kg}$ , a  $D$ -line transition frequency  $\omega_0=2\pi c/(852.4 \text{ nm})$ , and natural decay linewidth  $\gamma=2\pi \times 2.6 \text{ MHz}$ . To obtain strong entanglement, we advance these parameter values as reasonable:  $\Omega=2\pi \times 300 \text{ MHz}$  and  $\Delta=2\pi \times 15 \text{ GHz}$ . These give an upper population  $(\Omega/2\Delta)^2=0.0001$  and laser intensity  $I \approx 2\epsilon_0 c (\hbar\Omega/2ea_0)^2=90 \text{ W/cm}^2$ . Slowly moving cesium atoms can be prepared by an atomic fountain or by a magnetic trap. At a temperature of  $0.02 \text{ K}$ , the atom has a thermal speed  $\hbar\sigma_p/M=1.118 \text{ m/s}$ . Within the decay time  $\tau_R=0.612 \text{ ms}$ , the distance  $\Delta L$  traveled due to thermal motion is  $\Delta L=0.684 \text{ mm}$ . Therefore the atom will remain sufficiently long in the field if the laser has a beamwidth of several millimeters. Using these parameters, we get  $\eta_R \approx 5000$  and hence  $K \approx 1400$ , a huge increase over the value obtained for the spontaneous decay of sodium.

### IX. CONCLUSION

In summary, we have extended our previous studies of the photon-atom entanglement in spontaneous emission to Raman and Rayleigh scattering. We found strong analogies among the three processes, so that we could consider them in a single setting. We have provided a procedure to exploit their properties systematically. This procedure relies on the Schmidt method which not only gives a number (the Schmidt number, or participation ratio) to tell the “degree” of entanglement, but at the same time provides a discrete set of photon wave functions, whose individual elements pair up with their respective atomic counterparts. We have converted a continuous basis describing the Hilbert space into a countable one, which is effectively finite. The photon mode functions of the new basis can be uniquely and predictably localized in principle by projective measurement of the atom. Such an interpretation is possible only through the use of Schmidt decomposition.

In addition, the entanglement of the atom and the photon in the physical processes considered is found to be directly related to a single entanglement index  $\eta$ , which, in the case of Raman and Rayleigh scattering, can be controlled through the adjustment of the pump laser field strength and detuning. We have demonstrated that Rayleigh scattering using cesium atoms with reasonable laser parameters can give a Schmidt number as high as 1000, in contrast to the typically small  $K < 10$  in atomic spontaneous emission and parametric down-conversion.

Finally, it is noted that there is no experiment as far as the authors know that can investigate the properties of the atom or the photon in terms of their Schmidt modes, which demonstrate entanglement directly. In this paper, we have only dealt with the longitudinal momenta of the atom and photon. The transverse momentum distributions are expected to be detected more easily, and, with the Schmidt analysis, may find application in quantum imaging [18].

### ACKNOWLEDGMENTS

This work was principally supported by the DoD Multi-disciplinary University Research Initiative (MURI) program administered by the Army Research Office under Grant No. DAAD19-99-1-0215

[1] E. Schrödinger, *Nature (London)* **23**, 844 (1935).  
 [2] John S. Bell, in *Foundations of Quantum Mechanics*, edited by M. Bell, K. Gottfried, and M. Veltman (World Scientific, Singapore, 2001).  
 [3] A. Einstein, B. Podolsky, and N. Rosen, *Phys. Rev.* **47**, 777 (1935).  
 [4] W.H. Zurek, *Phys. Today* **44**, 36 (1991).  
 [5] M.A. Nielsen and I.L. Chuang, *Quantum Computation and Quantum Information* (Cambridge University Press, Cambridge, 2000).  
 [6] J.F. Clauser, M.A. Horne, A. Shimony, and R.A. Holt, *Phys. Rev. Lett.* **23**, 880 (1969); J.F. Clauser and M.A. Horne, *Phys. Rev. D* **10**, 526 (1974).  
 [7] A. Aspect, J. Dalibard, and G. Roger, *Phys. Rev. Lett.* **49**, 1804 (1982).  
 [8] T. Pfau *et al.*, *Phys. Rev. Lett.* **73**, 1223 (1994).  
 [9] M.S. Chapman *et al.*, *Phys. Rev. Lett.* **75**, 3783 (1995).  
 [10] C. Kurtsiefer *et al.*, *Phys. Rev. A* **55**, R2539 (1997).  
 [11] K.W. Chan, C.K. Law, and J.H. Eberly, *Phys. Rev. Lett.* **88**, 100402 (2002).  
 [12] C. Cohen-Tannoudji, J. Dupont-Roc, and G. Grynberg, *Atom-Photon Interactions* (Wiley, New York, 1992).  
 [13] The Schmidt theorem is equivalent to the singular value decomposition in matrix theory. Mathematical details can be

- found, for example, in A. Peres, *Quantum Theory: Concepts and Methods* (Kluwer Academic, Dordrecht, 1995).
- [14] H. Huang and J.H. Eberly, *J. Mod. Opt.* **40**, 915 (1993); **43**, 1891 (1996); C.K. Law, I.A. Walmsley, and J.H. Eberly, *Phys. Rev. Lett.* **84**, 5304 (2000).
- [15] R. Grobe, K. Rzǎżewski, and J.H. Eberly, *J. Phys. B* **27**, L503 (1994).
- [16] K. Rzǎżewski and W. Żakowicz, *J. Phys. B* **25**, L319 (1992).
- [17] See, for example, P.W. Milonni and J.H. Eberly, *Lasers* (Wiley, New York, 1988), Sec. 3.12.
- [18] See, for example, work in this direction by several groups: M.H. Rubin, *Phys. Rev. A* **54**, 5349 (1996); A. Gatti, E. Brambilla, L.A. Lugiato, and M.I. Kolobov, *Phys. Rev. Lett.* **83**, 1763 (1999); H.H. Arnaut and G.A. Barbosa, *ibid.* **85**, 286 (2000); A.F. Abouraddy, B.E.A. Saleh, A.V. Sergienko, and M.C. Teich, *ibid.* **87**, 123602 (2001).